

The effects of admixtures on the durability properties of phosphogypsum-based cementitious materials

Rusong Fu, Yuexian Lu, Lingling Wang, Hongfang An, Sihan Chen, Dewen Kong*

College of Civil Engineering, Guizhou University, Guiyang, Guizhou 550025, China



ARTICLE INFO

Keywords:
Phosphogypsum
Admixture
Durability property
Deterioration damage
Microscopic mechanism

ABSTRACT

This study involved proportionally blending beta-hemihydrate phosphogypsum (β -HPG) with raw phosphogypsum to prepare a phosphogypsum-based composite cementitious material (PGCM). The admixtures of quicklime (1–3%), cement (12–18%), and silica fume (5–9%) were selected to fabricate the PGCM mixture. The effect of each admixture on the durability performance of PGCM was evaluated using a single-factor experimental approach. The results showed that cement reduced significantly the dissolution rate and increased the strength coefficient, exhibiting the best effect on the antifreeze performance of PGCM. Quicklime and silica fume had no significant effect on the early antifreeze performance of PGCM but improved the later antifreeze performance. Moreover, the quicklime improved the weathering resistance of PGCM, whereas a high content of quicklime reduced the PGCM's strength coefficient. Silica fume improved the weathering resistance of PGCM in later phases, and cement had little effect on the weathering resistance of PGCM. Additionally, an increasing amount of cement significantly improved the water resistance of PGCM, and quicklime and cement significantly increased the length of PGCM specimens. Microscopic analysis showed that the generation hydration products mainly filled aggregate pores of raw phosphogypsum and enhanced raw phosphogypsum aggregates' interfacial adhesion, thereby improving the macroscopic mechanical and water resistance properties of PGCM. The findings on PGCM's durability properties can provide more theoretical foundations and technical supports for advancing phosphogypsum recycling.

1. Introduction

Adding phosphorus fertilizer to the soil has been regarded for a long time as the most effective way to increase soil phosphorus supply capacity and crop yield [1]. China has become the largest producer of phosphate fertilizer in the world due to the increasing scale of intensive agricultural planting, the expansion of urban scale, and the development of the residents' consumption level [2]. However, the large-scale production of phosphate fertilizers not only accelerates fossil energy consumption but also generates a large amount of phosphogypsum waste in the wet extraction of phosphoric acid [3].

Currently, phosphogypsum production is exploding globally, and the global production of phosphogypsum is estimated to reach 280×10^6 tonnes per year [4]. Due to the impact of various impurities in PG, only approximately 15% is recycled for construction materials, agricultural production, or cement production [5–8], and the rest of phosphogypsum is regarded as "waste" for centralized storage. The phosphogypsum stored in the open air will cause various problems, such as occupying a

large amount of land, seriously polluting the environment, and causing resource depletion [9]. Therefore, it is necessary to perform relevant research and seek low-cost, large-scale processing technology to consume a large amount of phosphogypsum [10].

Phosphogypsum has become a wide raw material owing to large reserves and low recycling costs. The application in building blocks [11, 12], wallboard fillers [13], or roadbed materials [14, 15] can effectively consume a large amount of phosphogypsum, which is beneficial to energy conservation and emission reduction. The main chemical composition of phosphogypsum is calcium sulfate dihydrate ($\text{CaSO}_4 \cdot 2\text{H}_2\text{O}$). It dissolves in water-ionized Ca^{2+} and SO_4^{2-} and can react with tricalcium aluminate (C_3A) to form calcium ettringite (Aft) [16, 17]. Currently, the most common approach in existing research is to mix various highly active admixtures into phosphogypsum to prepare phosphogypsum-based composite cementitious material to reach a particular strength. This method is inexpensive and can effectively improve the water-resistance of phosphogypsum and enhance its mechanical properties. However, many factors restrict the widespread

* Corresponding author.

E-mail address: dwkong@gzu.edu.cn (D. Kong).

application of PGCM, such as its low strength [18,19] durability properties [20–22]. Furthermore, the raw phosphogypsum contains a small amount of impurities[17,23] and radioactive substances[24,25], which limit the wide application of phosphogypsum. This is also a critical problem to increase the utilization rate of phosphogypsum as an environmental friendly green building material.

Many scholars have made efforts to prepare PGCM with high and stable strength. For example, volcanic ash is rich in silica (SiO_2), which can be activated by cement or slag to undergo a hydration reaction. Volcanic ash obtains high bonding properties and fills the internal pores of the substrate, thus improving mechanical properties and water resistance of PG [26–29]. After mixing phosphogypsum with cement and other admixtures, a cement binder with high activity can be formed. However, the curing effect of phosphogypsum is lower than that of natural gypsum[30], and the use of impure PG will lead to a decrease in the strength of cement clinker[31]. The excitation effect of washed phosphogypsum is stronger than that of ordinary PG[32]. Moreover, mixing calcined phosphogypsum with slag cement, fly ash, and quicklime can effectively enhance the compressive strength of the matrix[33, 34]. The results [19,35] showed that replacing fly ash with ordinary phosphogypsum reduced the compressive strength of the matrix by approximately 21%, and at the same time reduced the water resistance of the substrate. Additionally, the waste valorization conversion rate of phosphogypsum is larger in the phosphogypsum-steel slag-slag-limestone hybrid system [36], and its maximum admixture can reach 45%. Some scholars mixed industrial waste terracotta and rice husk ash with phosphogypsum as raw materials and finally found that phosphogypsum had the same performance as commercial gypsum. Some scholars mixed industrial waste red pottery and rice husk ash with phosphogypsum to become the raw material, and the study found that the performance of phosphogypsum was comparable to that of commercial gypsum [37].

The above research has played a beneficial role in promoting the comprehensive utilization of phosphogypsum. Many studies focused on the short-term mechanical properties of PGCM, and its mechanical and water resistance properties have a theoretical basis for molding. However, building materials have a long service life, and need to meet the requirements in the environments of long-term alternating humidity and temperature. phosphogypsum, as a building material, can be filled in the wall structure. Therefore, the long-term durability problem of PGCM is critical for its large-scale application in practical engineering.

The expansion and contraction of phosphogypsum building material limited its extensive application in building structures. Scholars have found that adding phosphogypsum to the mortar (self-leveling mortar) will increase the drying shrinkage and compact expansion of the matrix, resulting in a substantial increase in the shrinkage rate of the mortar [38]. Incorporating phosphogypsum into bricks can significantly increase their drying shrinkage[21,39]. After replacing part of the cement in the concrete with phosphogypsum, the expansion rate of the concrete will increase [40,41]. Excessive phosphogypsum content will lead to a higher expansion rate of gypsum products [36,42]. Some research has been conducted on the durability of composite materials mixed with phosphogypsum, such as load-bearing wall bricks [22], phosphogypsum concrete [43], cement mortar with phosphogypsum [19], fly ash-lime-gypsum bricks and hollow blocks [45], etc. It was found that adding phosphogypsum to the matrix reduced the wear resistance of the self-leveling mortar [38], improved the frost resistance of the matrix [22], enhanced the fire resistance of the matrix [43], reduced the heat insulation performance of the matrix [19], and improved Acid resistance of materials [44,45]. Phosphogypsum material exhibited poor water resistance, thus scholars conducted a lot of research to improve its water resistance. The current approach is incorporating polymers and organic materials into gypsum products to enhance water resistance [46–48]. At the same time, some scholars have improved the durability of gypsum by adding mineral admixtures[26,29,49–51] and have added fibers to enhance the frost resistance of phosphogypsum-based cementitious materials[52,53].

However, rare research focuses on the effects of admixtures on the durability of gypsum-based cementitious materials. In addition, there are even fewer reports on the interfacial adhesion between the internal components of materials and the evolution of hydration products under the erosion of complex environments. Therefore, this study investigated the effect laws of quicklime, cement, and silica fume, on the frost resistance, weathering resistance, water resistance, and dry shrinkage performance of PGCM using a single-factor test method. The macroscopic test phenomenon and the scanning results were further combined to jointly reveal the influence mechanism of each admixture on the properties of PGCM. The durability of PGCM was evaluated quantitatively, providing more theoretical foundations and references to promote the widespread and long-term engineering applications of phosphogypsum.

2. Materials and methods

2.1. Materials

The primary materials in the tests are: (1) Raw phosphogypsum is obtained from Guizhou Kailin Phosphogypsum Comprehensive Utilization Co., Ltd. It is in the form of off-white powder and needs to be air-dried before use and then used after sieving. (2) Beta-hemihydrate phosphogypsum ($\beta\text{-HPG}$) is made from raw phosphogypsum after calcination at a low temperature (160 °C) for 2 h, and the calcined PG needs to be taken out and sealed and aged for seven days before use. (3) Quicklime was purchased from Yibin Chuanhui Biotechnology Co., Ltd., and its active ingredient CaO content exceeded 96%. (4) The cement is market-purchased Conch PO 42.5 ordinary silicate cement. (5) Silica fume is taken from Gongyi Baichuan Environmental Protection Engineering Co., Ltd., and its SiO_2 content is above 97%. (6) Water reducing agent adopts 45% solid content of polycarboxylic acid liquid high-efficiency water reducing agent. (7) Gypsum retarder purchased from Shanghai Chenqi Chemical Technology Co. The microscopic morphologies of the main materials of the experiments are shown in Fig. 1. The main chemical compositions are listed in Table 1.

2.2. Experimental proportioning design

RPG has low cementitious property, while $\beta\text{-HPG}$ has well cementitious property and relatively high strength. The hydration reaction of $\beta\text{-HPG}$ generated ($\text{CaSO}_4 \cdot 2\text{H}_2\text{O}$) to fill the pores between RPG particles, improving the mechanical and water resistance properties of the mixture of raw phosphogypsum and $\beta\text{-HPG}$. However, $\beta\text{-HPG}$ was produced by the high-temperature calcination, consuming a lot of energy. Therefore, replacing part of raw phosphogypsum with $\beta\text{-HPG}$ is an efficient approach to enhance the properties of phosphogypsum-based cementitious materials. Furthermore, our previous research [54] studied the influences of the relative content between raw phosphogypsum and $\beta\text{-HPG}$ on the compressive strength, flexural strength and softening coefficient of phosphogypsum-based composite cementitious materials. The influences of the contents of three admixtures quicklime, cement and silica fume on strength and softening coefficient of phosphogypsum-based composite cementitious materials were also discussed. Therefore, this study investigated the effects of admixtures (Quicklime, Cement and Silica fume) on the durability properties of phosphogypsum-based cementitious materials using a single-factor experimental approach. When the influence of a certain admixture was investigated, the contents of the other two admixtures were fixed. The content of quicklime, cement and silica fume was respectively selected in the range of 1–3%, 12–18% and 5–9% according to our previous results [54], and a blank control group (without quicklime, cement and silica fume) was set to be a comparison group. The selection level of each admixture is shown in Table 2. The durability performance experiments were divided into the deterioration experiments (freeze-thaw cycle test and dry-wet cycle test) and the long-term performance

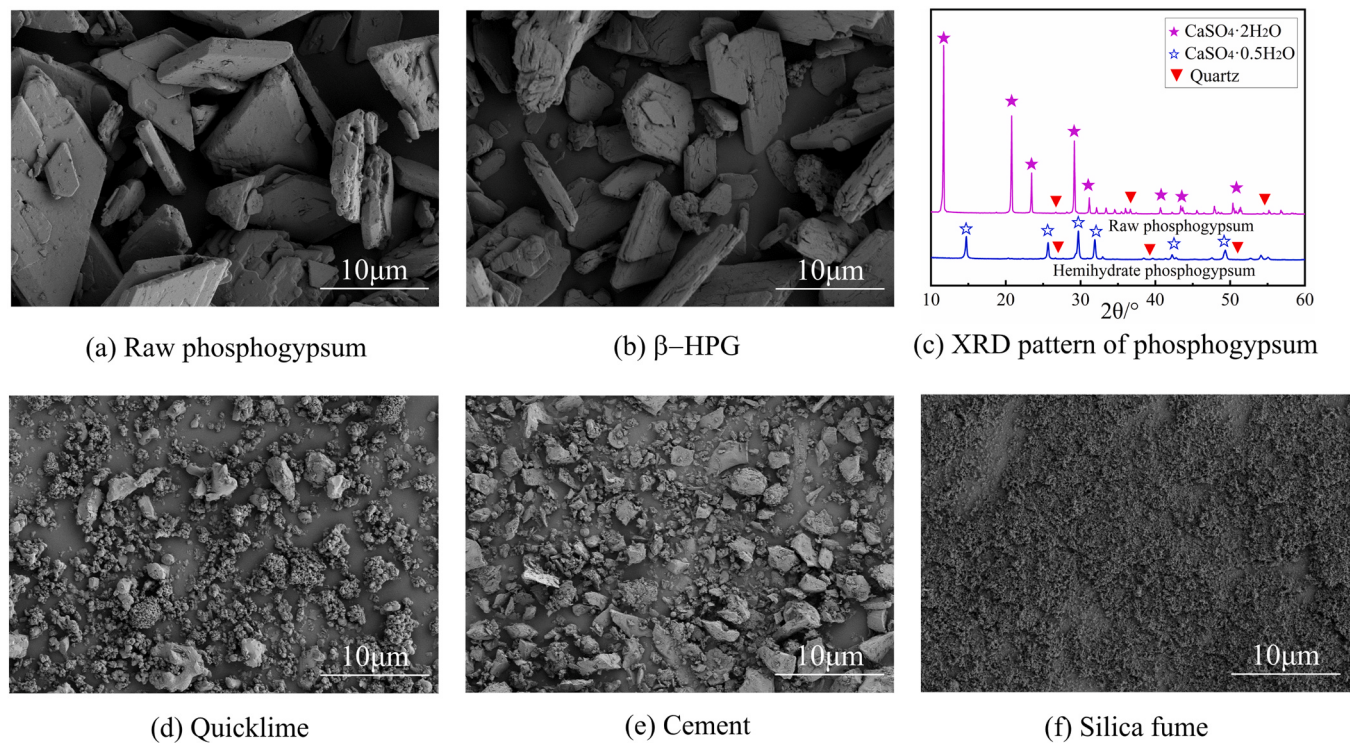


Fig. 1. Microscopic morphologies of experimental raw materials.

Table 1
Main chemical compositions of experimental raw materials.

Materials	SO ₃	CaO	SiO ₂	P ₂ O ₅	Fe ₂ O ₃	Al ₂ O ₃	K ₂ O	MgO
Raw phosphogypsum	55.28	39.52	2.68	0.89	0.37	0.30	0.07	-
β-HPG	53.60	41.84	2.71	0.86	0.38	0.29	0.07	-
Quicklime	0.29	96.78	0.52	0.01	0.11	0.15	2.05	0.01
Cement	3.96	61.71	19.90	0.17	4.46	5.16	1.20	1.73
Silica fume	0.46	0.48	97.60	0.04	0.07	0.81	0.22	0.21

Table 2
Factors and dosing levels in durability experiments.

Factor	Mixing ratio			
Quicklime (%)	0	1	2	3
Cement (%)	0	12	15	18
Silica fume (%)	0	5	7	9
Raw phosphogypsum: β-HPG	60%: 40%			

experiments (water resistance test and length shrinkage test). Deterioration experiments were used to understand the influences of admixtures on the antifreeze performance and weathering performance of PGCM. Long-term performance experiments were employed to explore the water resistance and length shrinkage law of PGCM. Solvation rate and strength coefficient of specimens after freeze-thaw cycle and wet-dry cycle, compressive strength of samples after long-term soaking in water and air curing to the specified age were determined. The length shrinkage scale was summarized when the sample is cured to the specified age.

2.3. Sample preparation and cure

The weighing method of the test material is as follows: the total mass of dry material remained constant, the weight of quicklime, cement, silica fume, water reducing agent was calculated referring to the total mass of dry material percentage, and water reducing agent proportion

was 1.5%. The total weight of the mixture of raw phosphogypsum and β-HPG was obtained by subtracting the total mass of quicklime, cement, silica fume from the total mass of dry materials, and the weight of raw phosphogypsum and β-HPG was calculated according to the experimental mix ratio (raw phosphogypsum:β-HPG=60%:40%). The mixing ratio of gypsum retarder is calculated based on 0.8% of the β-HPG dosage, and the water-cement ratio is 0.25.

The experimental material was placed in a mixer according to the weight of each material. The powdered materials were first mixed and stirred for 2 min to obtain a homogeneous mixture. After adding water, went slowly for 30 s, and then stirred rapidly for 90 s to get a uniformly mixed gypsum rheological body. Then the rheological body was poured into a mold of 40 × 40 × 160 mm³, and the rheological body was vibrated and compacted with a small vibrating table to eliminate air bubbles. After 24 h of curing in the natural environment, the samples were taken out and cured to the specified age under 20 ± 2 °C and relative humidity of 50 ± 5%. Finally, the specimens were removed and baked (40 ± 2 °C) in an oven until the quality was stable and tested for relevant properties.

2.4. Test contents and methods

2.4.1. Compressive strength

The mechanical strength of the sample was measured according to the GB/T17671 - 2021 Cement Mortar Strength Test Method (ISO Method). The absolute dry compressive strength was tested by an electro-

hydraulic servo pressure tester (YAD-300) with a maximum test load of 300 kN and a loading rate of 1 mm/s. The average compressive strength of three specimens was calculated as the final experimental result of the specimen.

2.4.2. Freeze-thaw cycle

The freeze-thaw cycle test was carried out concerning to the national standard *GB 50574–2010 Unified Technical Specifications for Application of Wall Materials*. Dry the sample to absolute dryness and measure its mass, and then put it in a freeze-thaw cycle tester for testing. The freeze-thaw regime was as follows. It was first frozen in the air at $-20 \pm 2^\circ\text{C}$ for 2 h and then immersed in water at $20 \pm 2^\circ\text{C}$ for three hours in one cycle. 30 cycles were set in the test, with five cycles as a level, and 6 cycle levels were set. After cycling to the specified grade, the specimen was removed and then baked in an oven at $60 \pm 5^\circ\text{C}$ until it was absolutely dry, and its quality and strength were measured. The dissolution rate and strength coefficient was calculated according to formulas (1) and (2), respectively.

$$C_{dt} = \frac{W_{d0} - W_{dt}}{W_{d0}} \quad (1)$$

Where: C_{dt} : freeze-thaw cycle dissolution rate; W_{d0} : the absolute dry mass of the specimen, g; W_{dt} : the mass of the specimen after t freeze-thaw cycles, g.

$$K_{dt} = \frac{R_{dt}}{R_{d0}} \quad (2)$$

Where: K_{dt} : freeze-thaw cycle strength coefficient; R_{d0} : initial dry compressive strength of the sample, MPa; R_{dt} : compressive strength of the sample after t freeze-thaw cycles, MPa.

2.4.3. Dry-wet cycle

The dry-wet cycle test referred to the national standard *GB/T 11969–2020 Methods for Performance Test of Autoclaved Aerated Concrete*. The sample was dried until reaching absolutely dry, and then cooled to room temperature to measure its mass. 30 cycles were performed in the test, with five cycles as a level, and six cycle levels were set. After cycling to the set number of times, the sample mass and compressive strength were removed and measured. The dissolution rate and strength coefficient was calculated according to formulas (3) and (4), respectively.

$$C_{gt} = \frac{W_{g0} - W_{gt}}{W_{g0}} \quad (3)$$

Where: C_{gt} is the dissolution rate of the dry-wet cycle; W_{g0} is the initial absolute dry mass, g; W_{gt} is the mass of the sample after t cycles, g.

$$K_{gt} = \frac{R_{gt}}{R_{g0}} \quad (4)$$

Where: K_{gt} is the dry-wet cycle strength coefficient; R_{g0} is the initial absolute dry compressive strength of the sample, MPa; R_{gt} is the compressive strength of the sample after t dry-wet cycles, MPa.

2.4.4. Long-term water resistance

The molded samples were cured for 28 days at $20 \pm 2^\circ\text{C}$ and $50 \pm 5\%$ relative humidity. Then the specimens were divided into two groups. One group of specimens was maintained in the air at the original temperature and humidity for further curing, and the other group of samples was cured in water at a temperature of $20 \pm 2^\circ\text{C}$. The compressive strength was measured at 7, 28, 60, 90, 120, 150, and 180 days, respectively.

2.4.5. Length shrinkage

The length shrinkage test was conducted concerning to *Test Methods for Basic Properties of Building Mortar (JGJ/T 70–2009)*. The direction of

the specimen test was marked after removing the mold so that the same position was always maintained for subsequent length test. The specimens were cured to 1d, 3d, 7d, 14d, 28d, 60d, 90d, 120d, 150d, and 180d and used SP-176 vertical mortar shrinkage meter to measure the length of the specimen. The specimen length shrinkage was calculated as follows. The initial length of each sample was taken as the reference value L_0 , the length of the sample at each age was L_d , and the length change value of each sample was recorded using $L_d - L_0$ at different ages.

2.4.6. Microscopic characterization

The microscopic morphology of the block sample was observed using a ZEISS Gemini 300 electron scanning microscope (SEM). The mineral phases of powdered materials were analyzed using a Bruker D8-Advance X-ray diffractometer (XRD). The hydration substances of sample were tested using an energy spectrometer.

3. Results and discussion

3.1. Freeze resistance

The frost resistance is an important indicator for the durability of building materials. Fig. 2 shows the damage patterns on the specimen surfaces after freeze-thaw cycles. Fig. 2(a)-(f) show the damage phenomena occurring on the surface of the specimen at different cycle times. From the graphs, we can find that at the beginning of the freeze-thaw cycle, the structural integrity of the sample is good; after ten cycles, the adhesion between the RPG aggregates inside the sample gradually decreases, and phosphogypsum begins to flake off; after 20 cycles, the structure of the sample is complete. The strength of the sample was destroyed, the corner raw phosphogypsum aggregates flaked off, and the sample volume became smaller; after 30 cycles, the strength of the sample was seriously lost. Only the middle skeleton played a structural support role, the outer raw phosphogypsum aggregate flaked off seriously, and the skin structure was relatively loose.

Fig. 2(g)-(j) show the apparent failure patterns of the samples. Analysis shows that the deterioration sequence of the specimen under the freeze-thaw cycles is as follows: (1) The skin flakes off at the beginning of the freeze-thaw cycle, exposing internal aggregates and holes to water. (2) During the warming stage, as the specimen is completely immersed in water, free water flows into the hardened body through the microcracks, and the exposed aggregate and phosphogypsum are gradually dissolved; the microcracks gradually expand, and the rate of water immersion becomes faster. (3) As the number of cycles increases, water erosion intensifies. In addition, the sample's surface begins to appear horizontal and vertical expansion cracks and continues to expand. The specimens eventually showed significant penetration cracks and suffered further erosion.

The mass dissolution ratio (freeze-thaw cycle dissolution rate) and strength coefficient (freeze-thaw cycle strength coefficient) can visually evaluate the frost resistances of phosphogypsum-based cementitious materials. Fig. 3 shows the change law of the dissolution rate and strength coefficient of PGCM sample after freeze-thaw cycles. It can be seen from Fig. 3(a) after 15 freeze-thaw cycles, the dissolution rate of the baseline group began to increase significantly. After adding quicklime, the dissolution rate of each group of samples was lower than that of the blank group, indicating that quicklime effectively improved the anti-freeze performance of the material, but the high content of quicklime had no obvious effect on the antifreeze performance of PGCM. Fig. 3(d) shows that quicklime can increase the strength coefficient of PGCM, and PGCM has the maximum strength coefficient at the content of quicklime of 2%.

Moreover, as shown in Fig. 3(b) and (e), the dissolution rate and the strength coefficient of the material (without quicklime, cement and silica fume) changes rapidly with increasing the number of freeze-thaw cycles. However, PGCM exhibits relatively slow change under different numbers of freeze-thaw cycles. These phenomena indicate that cement

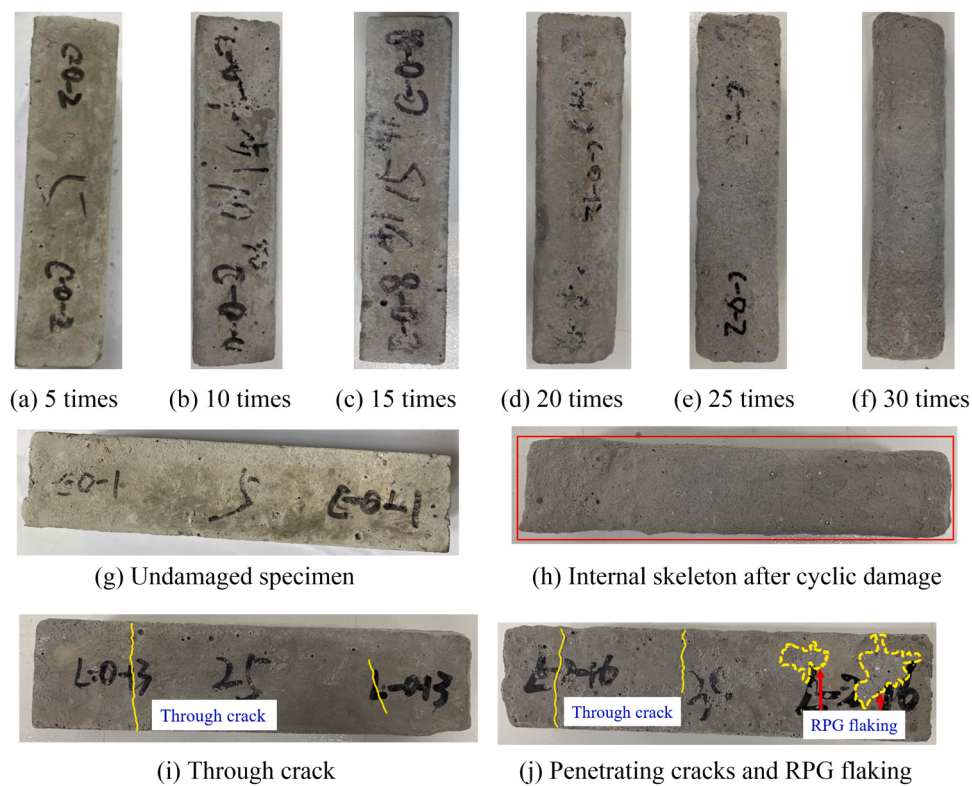


Fig. 2. Macroscopic damage pattern of PGCM after freeze-thaw cycles.

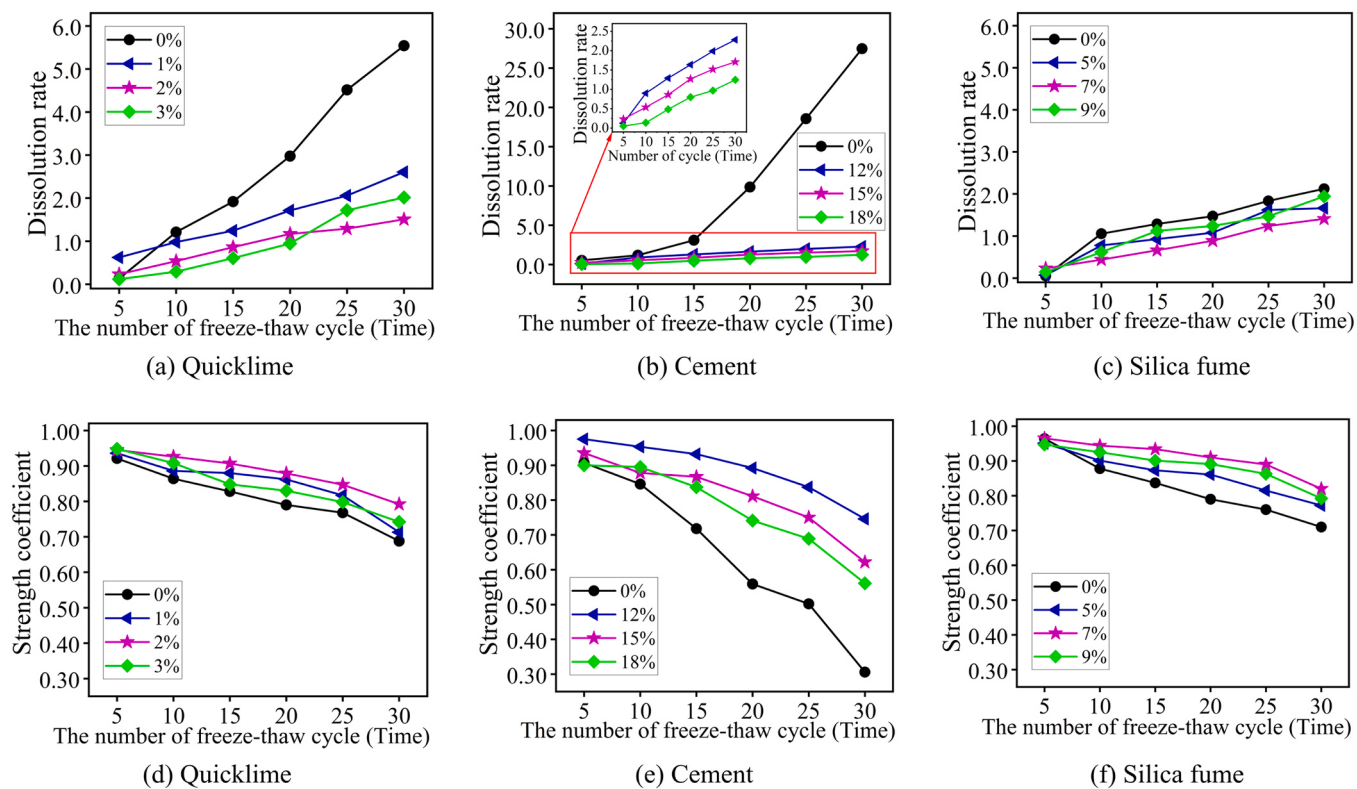


Fig. 3. Dissolution rate and strength coefficient of PGCM after freeze-thaw cycle test.

has more significant influence on dissolution rate and the strength coefficient of PGCM. When the cycle was 20 times, the dissolution rate of the blank group sample exceeded the failure standard (the specimen

reached the failure standard when the dissolution rate was >5%). When the cycle was 30 times, the dissolution rate of the sample in the blank control group was as high as 27.47%, and the strength coefficient of the

sample was extremely low. According to the analysis consequences in Fig. 3(b) and (e), cement is the key factor for improving the antifreeze performance of PGCM.

It can be seen from Fig. 3(c) and (f) that silica fume has little effect on the dissolution rate and strength coefficient of PGCM. When the number of cycles is 5, the antifreeze performance of the sample without silica fume is almost the same as that of the sample mixed with silica fume. When the number of cycles increases to 10, silica fume exhibits the improvement effect on the antifreeze performance of PGCM. This phenomenon shows that silica fume has no improvement effect on the early antifreeze ability of PGCM, but has effective improvement in the later antifreeze ability of PGCM. The improvement becomes more evident with the increase in the number of cycles. Therefore, it is advisable to control the dosage of silica fume at about 7%, when PGCM is applied to an environment of high frost resistance.

3.2. Weathering resistance

The appearance of the sample after the dry-wet cycle is shown in Fig. 4. From Fig. 4(a)-(f), the damage degree of the PGCM sample under the dry-wet cycle is lower than that of the freeze-thaw cycle, and the surface of each group of test pieces is less eroded.

Fig. 4(g)-(j) show the damage morphology of the sample after the loading of alternating wet and dry erosion. When the number of cycles is low, the sample has good structural integrity, and its internal skeleton is not damaged; when the number of cycles reaches 20, some short but disconnected cracks appear on the surface of the sample, and majority cracks are transverse. After 30 cycles, raw phosphogypsum flakes off from the surface of the sample in a large area, the internal skeleton is exposed, and the corners of the block fall off. The damage area of the sample is relatively extensive after 30 cycles.

After dry-wet cycles, the damage process of PGCM can be divided into two stages: the immersion stage and the drying stage. In the

immersion stage, the loose and porous interior of PGCM caused significant micro-cracks between the internal aggregates, which make free water easy to enter and exit the hardened body. Water penetrates the matrix along the micro-cracks when the sample is soaked. Moreover, the hydration products of cement and silica fume are easily decomposed in water, thus the cracks are further elongated and widened. In the drying stage, when the sample is dry, water molecules will seep out along the pores and micro-cracks of the gypsum particles, and the dissolution of hydration products and dihydrate gypsum is accelerated during this process. The flowing water molecules took these substances out together, and scoured the micro aggregates around the cracks. As the scouring action further expands, the new secondary cracks were generated inside the matrix, and the strength of the specimen is further weakened.

Fig. 5 shows the influences of different admixtures on the dissolution rate (dry-wet cycle dissolution rate) and strength coefficient (dry-wet cycle strength coefficient) of the PGCMs after the dry-wet cycles. Fig. 5 (a) and (d) indicate that quicklime can effectively reduce the dissolution rate of PGCM and improve its strength at the quicklime content of 1% and 2%. When the number of cycles reached 25, the specimens with 2% quicklime had better weathering resistance, while the samples with 3% quicklime showed poor weathering resistance. Consequently, when the number of dry-wet cycle reaches 15, PGCM with 2% quicklime has lower dissolution rate and higher strength coefficient. Therefore, it is clear that the quicklime dosage of 2% is beneficial in improving the weathering resistance of PGCM under dry-wet cycle condition.

It can be found from Fig. 5(b) and (e) that, cement increases the dissolution rate and the strength coefficient of the PGCM. Moreover, the enhancement effect of cement on the strength coefficient of PGCM is related to the number of cycles as shown in Fig. 5(e). Below the dry-wet cycles of 15, the strength coefficient of PGCM is the highest when the cement dosing is 12%, and the strength coefficient of PGCM with cement dosing of 15% is the highest above 15 cycles. The strength coefficient of PGCM with cement dosing of 18% is relatively lower than that at the

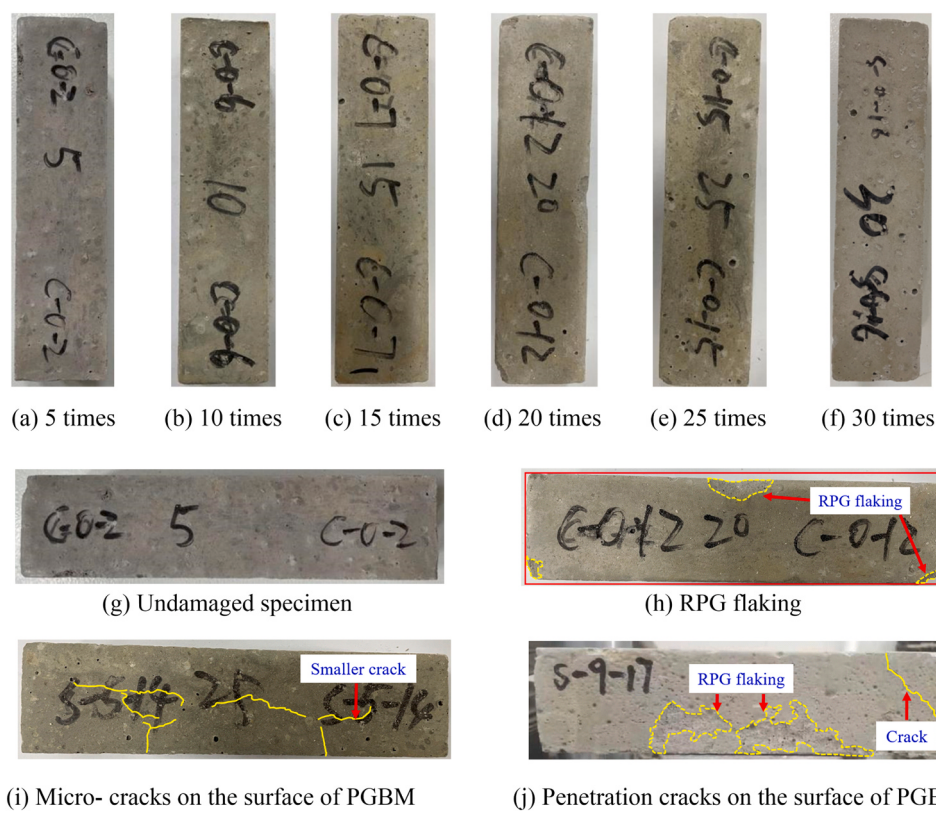


Fig. 4. Macroscopic damage pattern of PGCM after dry-wet cycles.

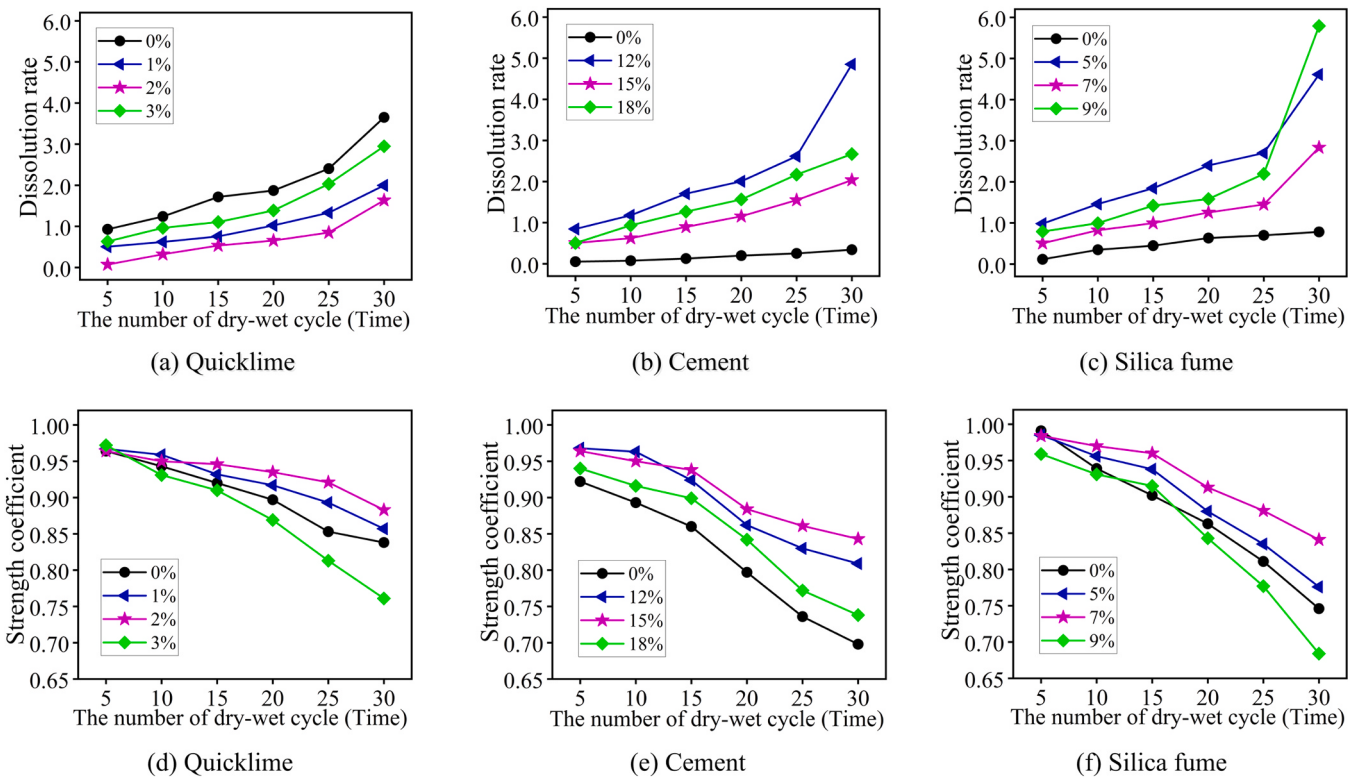


Fig. 5. Dissolution rate and strength coefficient of PGCM under the dry-wet cycle.

cement dosing of 12% and 15%. These above phenomena show that cement significantly improves the mechanical property of PGCM, but significantly decreases the antifreeze performance of PGCM. This is because at the large dosing of cement, the hydration reaction generates the calcium alumina crystals inside the hardened body of PGCM, which squeezes the surrounding aggregates and increases the number of microcracks, reducing the weathering resistance of PGCM.

From Fig. 5(c) and (f), silica fume increases the dissolution rate, and increase the strength coefficient of the PGCM at the dosage of 5% and 7%. Throughout the hydration process, the silica fume involved in the hydration reaction of PGCM and exhibited no intense volcanic ash activity after a certain amount, weakening its chemical effect. Fig. 5(c) shows that the dissolution rate of the specimen fluctuates significantly above 20 cycles. This consequence is accordance with the apparent phenomenon in Fig. 4(e), in which the surface of the sample appears obvious microcracks under 25 cycles. This indicates that the crack expansion inside the PGCM starts to increase rapidly above the cycle number of 20. The more crack diffusion can make silica fume particles contact with water and thus undergo a secondary hydration reaction. Therefore, the dissolution rate value increases rapidly above the cycle number 20. As a result, PGCM with 15% silica fume exhibits relatively better mechanical property and weathering resistance when the dosage of silica fume changes from 12% to 18%.

Moreover, the flaking material from PGCM specimen was collected and dried after the deterioration experiment (freeze-thaw cycle and wet-dry cycle) to clarify its component using an XRD inspection. The XRD result is shown in Fig. 6, which states that the mineralogy of the flaking material is $\text{CaSO}_4 \cdot 2\text{H}_2\text{O}$, same as that of raw phosphogypsum. Therefore, this conclusion is verified that the flaking material of the PGCM specimen after the deterioration experiment is raw phosphogypsum.

3.3. Long-term water resistance

Fig. 7 shows the compressive strength variation trend of PGCM samples under different curing ages in air and water. Fig. 7(a) shows that

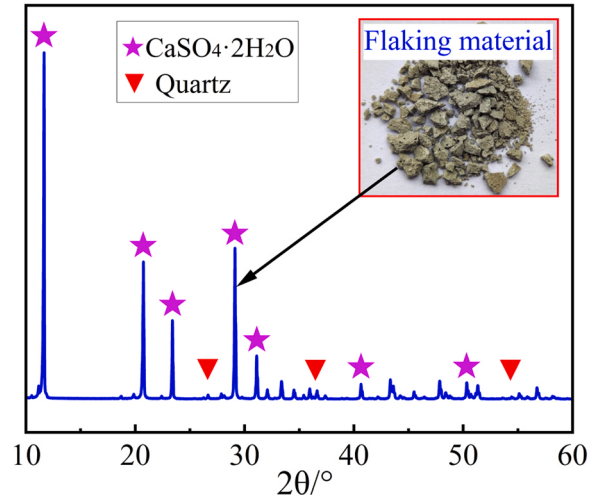


Fig. 6. XRD pattern of the flaking material.

when the sample is cured in the air, the compressive strength of the sample with 1% quicklime has a slight decrease after 60 days of curing age, the compressive strength of the sample with 2% and 3% quicklime increases with the extension of the curing age, and the highest compressive strength reaches 30.61MP. Moreover, in the early stage of curing (<60 days), the content of quicklime had no significant effect rule on the compressive strength, owing to the influence of hydration reaction. In the early curing stage, the higher content of quicklime absorbed water and expands, softening the specimens and resulting in a relatively lower initial strength. However, as the hydration reaction continues in the later curing stage (>60 days), the strength of PGCM increased with the increase of the quicklime content from 1% to 2%. However, when the quicklime content was greater than 2%, the unreacted residual

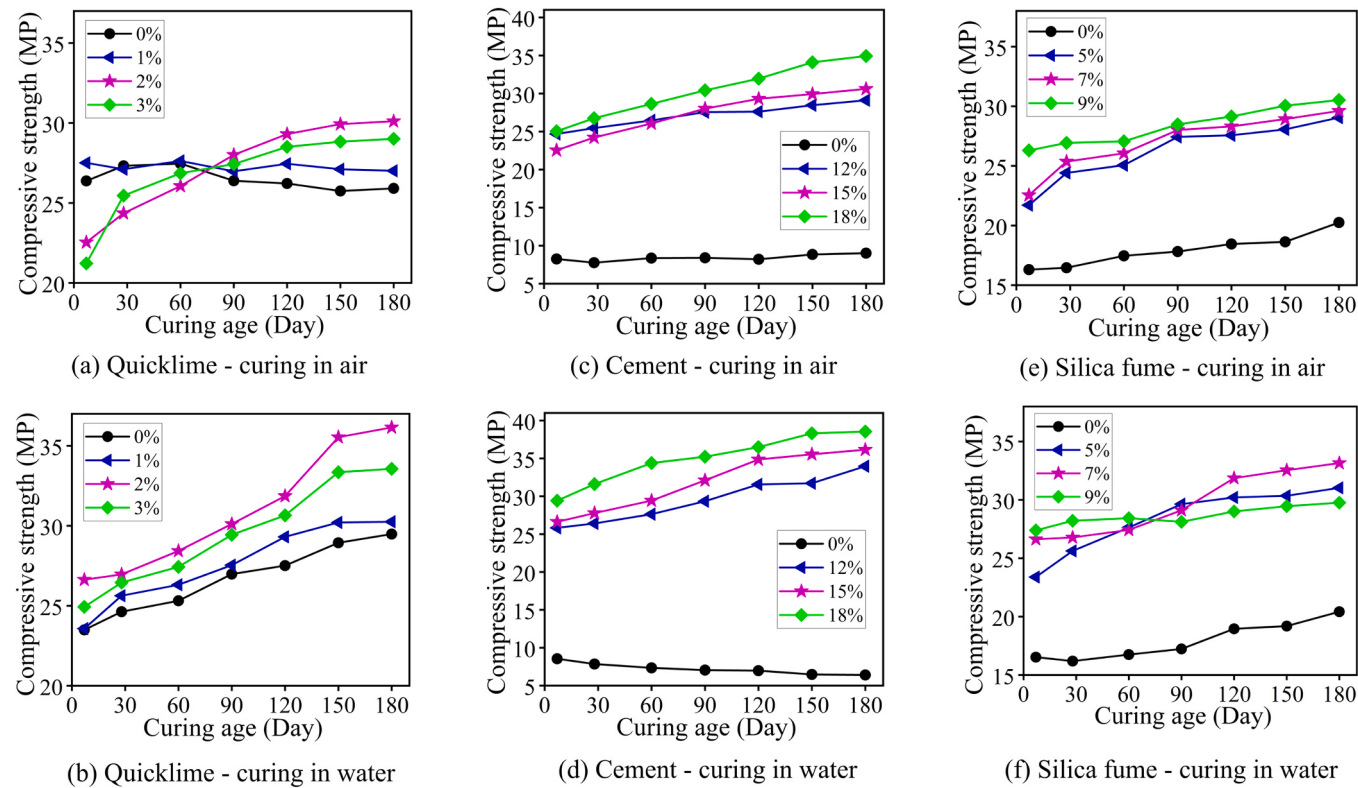


Fig. 7. Compressive strength of PGCM at each age under different curing methods.

quicklime contained in the matrix reduced the strength of PGCM. Under curing in water, the compressive strength of the PGCM specimen increases with the extension of curing age, and is higher than the value of the blank control group. Moreover, the compressive strength of PGCM cured in water has a slight increase after the curing age of 150 days.

From Fig. 7(c) and (d), for the specimen without cement, the compressive strength has no significant increase in air, and the compressive strength has a decrease in water with the extension of the curing age. At the curing age of 180 days, the maximum decrease of compressive strength is 2.13 MPa. After adding cement, the compressive strength of the specimen increases with the increase in curing age in both curing methods, and the improvement in compressive strength is higher in water curing condition. The main reason is that the water-filled environment accelerates the hydration rate of cement, resulting in more calcium-alumina crystals, which increases the compactness of the matrix and increases the compressive strength of PGCM. However, in air curing condition, specimen with 15% cement exhibited relatively lower compressive strength within 60days. This was because the strength of PGCM was dependent on the hydration products and hydration degree. Cement underwent a rapid hydration reaction to generate excess hydration products in a strong alkali environment, which encapsulated raw materials of raw phosphogypsum and β -HPG [16]. Additionally, the existing studies [55,56] observed that calcium hydroxide ($\text{Ca}(\text{OH})_2$) particles adsorbed on the surface of gypsum dihydrate crystals. These above phenomena prevent further hydration reactions between cement and raw materials. Therefore, the more internal gel formation of PGCM with a cement content of 15% can reduce the hydration of the mixtures, causing the lower compressive strength at the early stage.

Additionally, it can be concluded from Fig. 7(e) and (f) that the dosage of silica fume has a slight influence on the compressive strength of PGCM, which is attributed to the hydration involvement of silica fume in the hardened body. An important discovery can be summarized by analyzing the compressive strength of samples under different curing

methods. Silica fume leads to the generation of a gel inside the sample, which can resist water erosion, thereby enhancing the water resistance of PGCM. Therefore, the compressive strength of PGCM has a slight difference under air and water curing methods. However, at the silica fume content of 9%, the residual silica fume particles did not participate in the reaction in the later stages of curing in water and did not play a filling role, which reduced the bonding force between raw phosphogypsum particles. This caused a significant reduction in the compressive strength of PGCM at the silica fume content of 9%, compared with the compressive strength of PGCM with 5% and 7% silica fume.

3.4. Shrinkage in length

The length variations of the specimens under different maintenance ages are shown in Fig. 8. According to Fig. 8, the contraction of PGCM can be roughly divided into three stages. (1) In the first stage from 1 to 7 days, the reaction system is in a water-saturated environment, and each aggregate will absorb water, causing its volume to expand rapidly, thus the length of the specimen under this stage varies greatly. (2) The second stage is from 7 to 60 days. At this stage, the hydration reaction inside the sample continued, the free water continued to be consumed and volatilized, and the volume of each aggregate decreased slowly. Combining the above two action mechanisms, the volume and length changes of the samples developed steadily. (3) The third stage is after 60 days. At this stage, the hydration reaction stagnates due to the lack of water inside the material, so the strength development and length change of the specimens tend to be stable.

It can be seen from Fig. 8 that quicklime and cement can increase the length of the PGCM sample, and silica fume has little increase effect on the length of the sample, compared with the blank group. The length of specimen without quicklime shrinks under each maintenance age, the length shrinkage of specimen reduced after mixing with 1% quicklime. After mixing with 2% and 3% quicklime, the length of sample grows under each maintenance age, which is caused by the increase of water

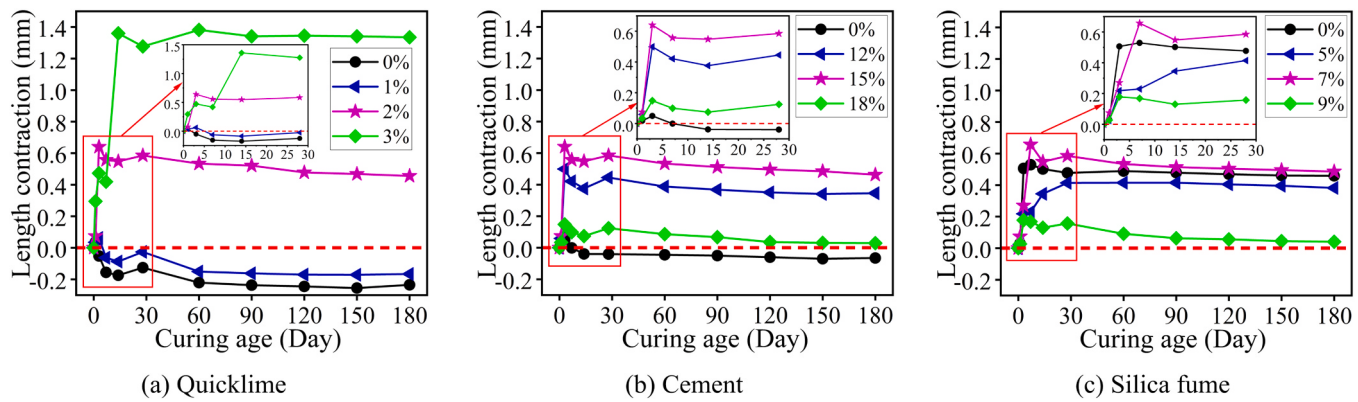


Fig. 8. The length variation of PGCM specimen at different curing ages.

absorption and swelling of quicklime and the generation of hydration products. When no cement is added, the length of the sample decreases with the increase of curing age. Cement increases the expansion degree of PGCM, and the length of the sample has a maximum increase at the cement content of 15%. This was related to the following reasons: cement caused the increase of the hydration products in the internal pores and cracks in the hardened body and continuously squeezed the surrounding aggregates, thereby increasing the length of the PGCM. The length of the sample without silica fume increases due to the expansion of quicklime and water absorption. After adding silica fume, the quicklime activated the silica fume, increasing the consumption of quicklime and having a negative effect on the sample length growth.

3.5. Microanalysis

3.5.1. Damage mechanism

The bonding support between hydration products inside the material provides the macroscopic mechanical strength of the material. Materials appeared different degrees of damage under the dry-wet cycles. Fig. 9 shows the internal damage process of the PGCM after being subjected to the erosion of the dry-wet cycle.

The hydration reaction of PGCM is an ongoing process. The PGCM produces fewer floccules in the early hydration stage, forming more micropores. In the later stage, the free water inside the matrix continued to evaporate, and the hydration reaction slowed down, resulting in an increase in pores inside the specimen, which provided conditions for later water storage. When the sample is soaked in water, the internal and external micropores continue to accumulate water, which causes the unreacted quicklime in the material to absorb water and expand, resulting in expansion stress. The pores and microcracks in the specimen further expanded under the expansion stress. During the dry process, the evaporation of free water inside the pores and microcracks makes the material in a state of dehydration, generating shrinkage stress. This results in further widening of the cracks on the surface of the hardened body or more microcracks, and finally a network crack phenomenon appears. Under the alternating action of dry and wet environments for a

long time, shrinkage and expansion stress also appear alternately. Alternating stress gradually increases the width and length of the crack, and multiple independent pores are finally connected to form larger and longer penetrating cracks. These cracks reduce the adhesion between the aggregates within PGCM, which decrease the specimens' mechanical properties and water resistance.

Water absorption and expansion is a remarkable characteristic of porous materials. Fig. 10 shows that a large amount of free water is stored in the holes of the PGCM specimen after the freeze-thaw cycle test in water. In the subzero temperature environment, the free water in the large pores freezes before the free water in the small pores, resulting in an increase in the ion concentration inside the large pores and a concentration difference with the small pores. As a result, free water in the small pores flows to the large pores, resulting in a constant increase in the hydrostatic pressure in the large pores. In addition, the free water inside the pores expands in volume during the freezing process, forcing the unfrozen water to develop hydrostatic pressure P against the capillary wall. The capillary pores become enlarged under pressure P and the

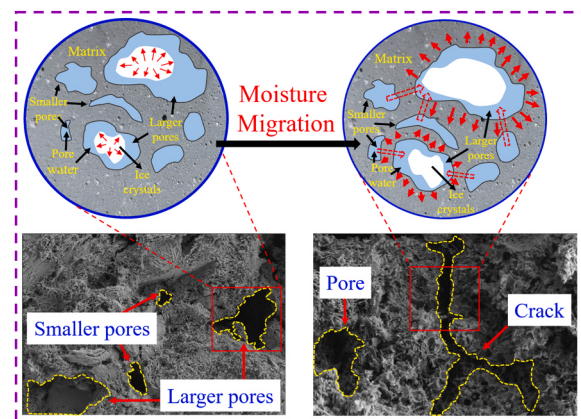


Fig. 10. Damage mechanism of PGCM after freeze-thaw cycle experiment.

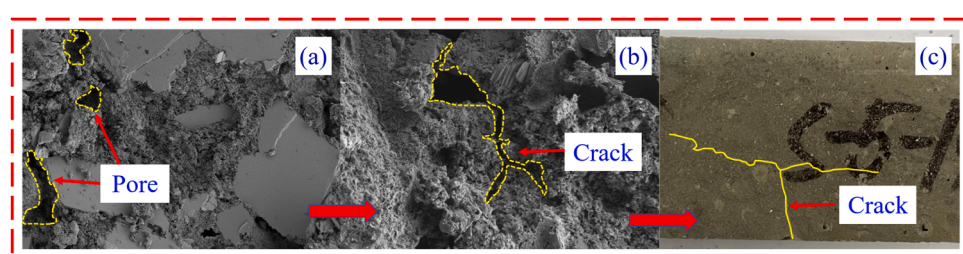


Fig. 9. Damage mechanism of PGCM after dry - wet cycle experiment.

damage of the specimen accumulates. In the above-zero temperature environment, the crystal water in the pores of PGCM melts slowly. Since the specimen is in a water-saturated environment, the pores expanded by the crystal water and no longer shrink, and the next cycle is continuously squeezed and expanded by the crystal water. Under the cyclic action of positive and negative temperature environments, the macroscopic physical and mechanical properties of PGCM continue to deteriorate, eventually leading to material failure.

3.5.2. Hydration products

Three main substances were generated by the hydration of each admixture in this study from Fig. 11(d)-(e). Three main substances are respectively energy spectra of ettringite (Aft), calcium silicate hydrate gel (C-S-H), and calcium sulfate dihydrate crystal ($\text{CaSO}_4 \cdot 2\text{H}_2\text{O}$). As shown in Fig. 11(a), after the hydration reaction, a large amount of C-S-H bonded to the surface of PG particles, gradually covering and wrapping the gypsum particles. The surface of phosphogypsum particles surrounded by gel was covered again by new hydration products, thus forming a new gel adhesive layer, and this cycle eventually caused phosphogypsum particles to be wholly wrapped by hydration products. The consolidation process of hydration products on PGCM is as follows: when the matrix began to hydrate, many C-S-H flocs bonded together and formed larger fillers attached to the surface of phosphogypsum particles. At the same time, Aft crystals are constantly produced and interspersed between C-S-H to form complexes. These complexes can provide attachment points for the sedimentation of CaSO_4 crystals, thereby accelerating the crystallization rate of dihydrate gypsum. A small amount of silica fume particles not involved in hydration can also be seen in the figure. The above substances are interconnected and polymerized to form larger cluster gel polymers and adhere to the surface of phosphogypsum particles, which improves the compactness of PGCM. This is a main reason to improve the macroscopic mechanical properties and water resistance of PGCM. Fig. 11(b) shows that a new crystal-gel combination is formed under the dense gel bonding degree. The surface of the combination has strong hydrophobicity, which can prevent water from penetrating the

interior along the micro-cracks, improving the water resistance of PGCM.

Fig. 12 (a) and (b) show that the peak of the mineral phase diagram for PGCM sample is still relatively high after the erosion test. This indicates that although the erosion test reduce the content of hydration products, the ion balance of the solution inside the matrix is affected, and the admixture continues to dissolve in water and release more mineral ions to form new hydration products. As a result, new hydration products are generated continuously when the number of cycles increases, although the adhesion of the aggregates within PGCM is affected. The calcium alumina crystals and hydrated calcium silicate gels that are hydrolyzed due to erosion tests are compensated, and the interfacial adhesion between the aggregates inside PGCM is continuously enhanced so that the macroscopic mechanical properties and water resistance of PGCM remain stable. The XRD results of the specimens at each age under different maintenance environments are shown in Fig. 12 (c) and (d). The peak value of Aft is lower, indicating that the dissolution of dihydrate gypsum is slow in the early hydration stage, resulting in less Aft formation. With the increase of curing age, the peak value of Aft become higher, and the peak value of dihydrate gypsum decreases. It shows that the dissolution rate of dihydrate gypsum gradually increases with the prolongation of the curing period, and the hydration degree of each admixture inside the material becomes more and more complete.

4. Conclusion

(1) Three admixtures of quicklime, cement and silica fume have effects on the freeze resistance of PGCM. The effects of the admixture dosage and the number of freeze-thaw cycle on the dissolution rate and the strength coefficient of PGCM were discussed quantitatively. Quicklime effectively improves the freeze resistance of PGCM, and PGCM has the better dissolution rate strength coefficient at the content of quicklime of 2%. Cement has more significant influence on dissolution rate and the strength

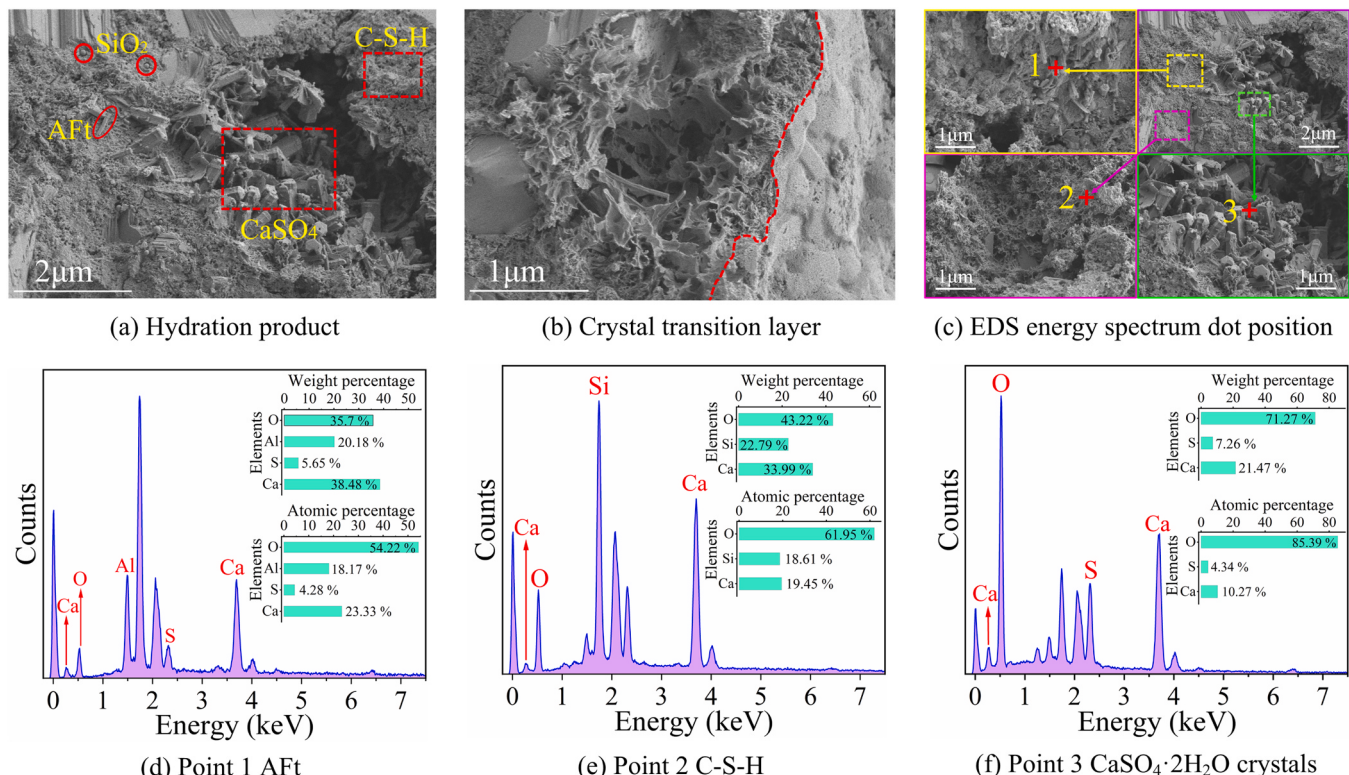


Fig. 11. Main hydration products of PGCM and their distribution positions.

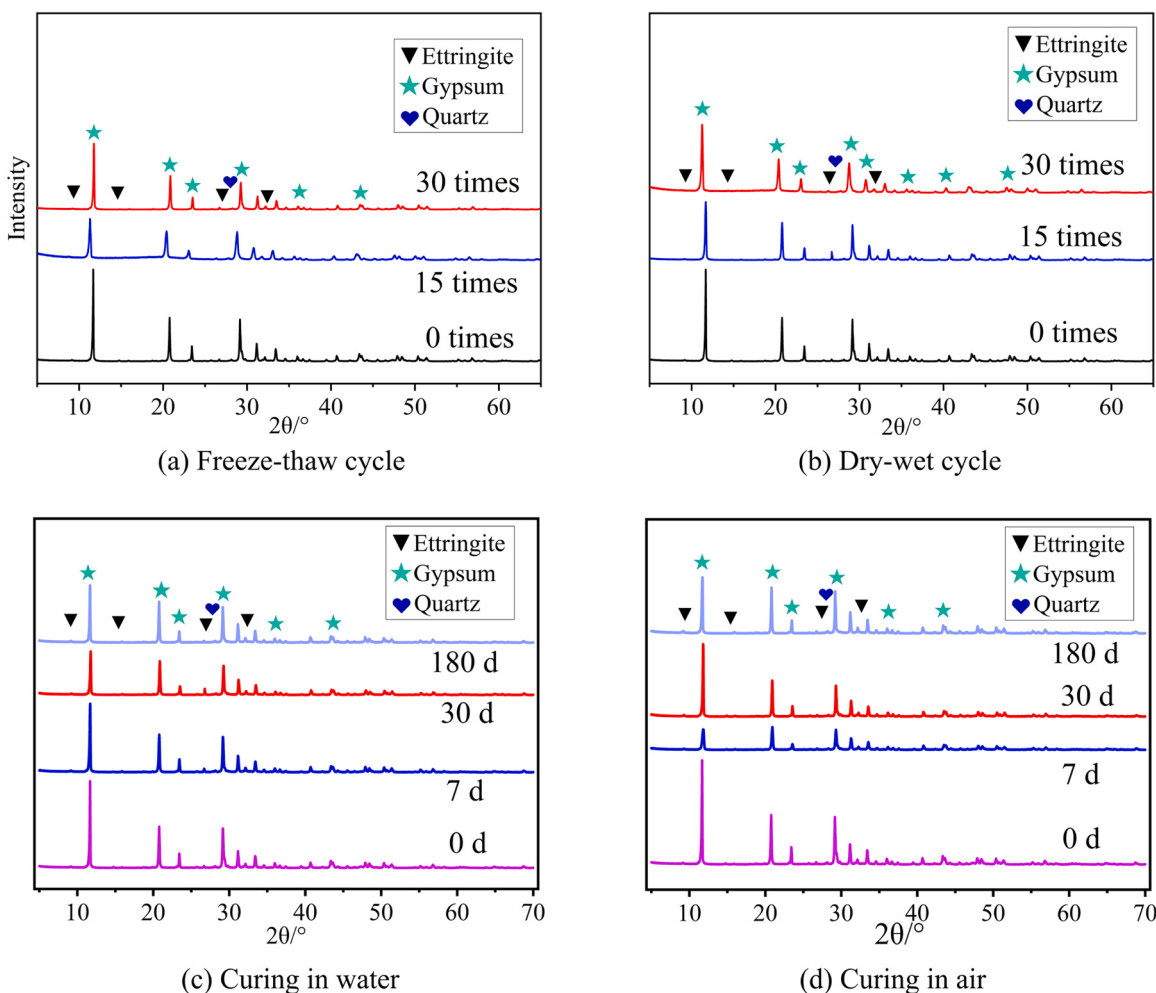


Fig. 12. The mineral phase of PGCM under different conditions.

- coefficient of PGCM. Silica fume has no improvement effect on the early antifreeze ability of PGCM, but has effective improvement in the later antifreeze ability of PGCM. Moreover, PGCM appears more significant damage with the increase in the number of Freeze-thaw cycles.
- (2) The dry-wet cycle resulted in less damage to the PGCM, and the overall deterioration of the sample was lower than that of the freeze-thaw cycle. Quicklime can enhance the weathering resistance of PGCM, but excessive quicklime decreases the strength coefficient. Cement is not conducive to improving the weathering resistance of PGCM, and high dosage of cement admixture increases the dissolution rate and reduces the strength coefficient. Silica fume can improve the weathering resistance of PGCM in the later stage.
- (3) Three admixtures of quicklime, cement and silica fume have more significant improvement effects on the compressive strength of PGCM in water curing condition than that in air. The quicklime can improve the later strength, cement can significantly increase the hardened body's density and the PGCM' strength, and 7% silica fume enhances the compressive strength of PGCM after 90 curing ages.

- (4) According to the evaporation of water inside the hardened body and the continuous production of hydration products, the expansion and contraction of the PGCM sample can be divided into three stages. The first stage is 1–7 days, the second is 7–60 days, and the third is 60 days later. Quicklime and cement can

reduce the shrinkage of PGCM, whereas silica fume has little effect on the shrinkage of PGCM.

- (5) Microscopic analysis shows that the PGCM contains mainly three mineral components, phosphogypsum, Aft, and quartz. Aft is a hydration product and increases with the prolongation of curing age. SEM and energy spectrum analysis show that the internal hydration products of PGCM hardened body mainly include ettringite, calcium silicate hydrate gel, and calcium sulfate crystals. These three hydration products are bonded with each other to form agglomerates, which fill the pores and enhance the interfacial adhesion, thereby improving the macroscopic mechanical properties and water resistance of PGCM.

CRediT authorship contribution statement

Rusong Fu: Writing – original draft, Validation, Methodology, Investigation, Data curation, Conceptualization. **Yuxian Lu:** Methodology, Conceptualization. **Lingling Wang:** Writing – review & editing, Resources. **Hongfang An:** Visualization, Software. **Sihan Chen:** Validation, Software. **Dewen Kong:** Writing – review & editing, Funding acquisition.

Declaration of Competing Interest

The authors declare that they have no known competing financial interests or personal relationships that could have appeared to influence the work reported in this paper.

Data availability

Data will be made available on request.

Acknowledgments

This work was supported by the National Natural Science Foundation of China (Grant Nos. 52168027 and 51968009); Guizhou Provincial Science and Technology Project (Grant No. [2020]1Y244), and Guizhou Province Science and Technology Support Project (Grant No. [2022]027).

References

- [1] J.X. Du, T.F. Han, X. Qu, L. C.B. Ma, K.L. Liu, J. Huang, Z. Shen, L. Zhang, L.S. Liu, J.H. Xie, H.M. Zhang, Spatial-temporal evolution characteristics and driving factors of partial phosphorus productivity in major grain crops in China, *J. Plant Nutr. Fertil.* 28 (02) (2022) 191–204.
- [2] F.F. Zhang, Q.S. Wang, J.L. Hong, W. Chen, C.C. Qi, L.P. Ye, Life cycle assessment of diammonium-and monoammonium-phosphate fertilizer production in China, *J. Clean. Prod.* 141 (2017) 1087–1094.
- [3] R.Q. Jia, Q. Wang, T. Luo, Reuse of phosphogypsum as hemihydrate gypsum: the negative effect and content control of H_3PO_4 , *Resour. Conserv. Recycl.* 174 (2021), 105830.
- [4] M.V. Silva, L.R. de Rezende, M.M.D. Mascarenha, R.B. de Oliveira, Phosphogypsum, tropical soil and cement mixtures for asphalt pavements under wet and dry environmental conditions, *Resour. Conserv. Recycl.* 144 (2019) 123–136.
- [5] A.M. Rashad, Phosphogypsum as a construction material, *J. Clean. Prod.* 166 (2017) 732–743.
- [6] L. Reijnders, Cleaner phosphogypsum, coal combustion ashes and waste incineration ashes for application in building materials: A review, *Build. Environ.* 42 (2) (2007) 1036–1042.
- [7] H. Tayibi, M. Choura, F.A. López, F.J. Alguacil, A. López-Delgado, Environmental impact and management of phosphogypsum, *J. Environ. Manag.* 90 (8) (2009) 2377–2386.
- [8] F.A. Lopez, M. Gazquez, F.J. Alguacil, J.P. Bolivar, I. Garcia-Diaz, I. Lopez-Coto, Microencapsulation of phosphogypsum into a sulfur polymer matrix: physicochemical and radiological characterization, *J. Hazard. Mater.* 192 (1) (2011) 234–245.
- [9] I. Sengupta, P.K. Dhal, Impact of elevated phosphogypsum on soil fertility and its aerobic biotransformation through indigenous microorganisms (IMO's) based technology, *J. Environ. Manag.* 297 (2021), 113195.
- [10] T.L. Roberts, A.E. Johnston, Phosphorus use efficiency and management in agriculture, *Resour. Conserv. Recycl.* 105 (2015) 275–281.
- [11] J. Zhou, D.X. Yu, Z. Shu, T.T. Li, Y. Chen, Y.X. Wang, A novel two-step hydration process of preparing cement-free non-fired bricks from waste phosphogypsum, *Constr. Build. Mater.* 73 (2014) 222–228.
- [12] L. Ajam, A.B. Hassen, N. Reguigui, Phosphogypsum utilization in fired bricks and Radioactivity assessment, *J. Build. Eng.* 26 (2019), 100928.
- [13] S. Hu, L. Zhou, Y. Huang, Experimental investigation on the seismic performance of phosphogypsum-filled cold-formed thin-walled steel composite walls, *Thin-Walled Struct.* 186 (2023), 110664.
- [14] S. Meskini, I. Mechoua, M. Benmansour, T. Remmal, A. Samdi, Environmental investigation on the use of a phosphogypsum-based road material: radiological and leaching assessment, *J. Environ. Manag.* 345 (2023), 118597.
- [15] W.G. Shen, M.K. Zhou, W. Ma, J.Q. Hu, Z. Cai, Investigation on the application of steel slag-fly ash-phosphogypsum solidified material as road base material, *J. Hazard. Mater.* 164 (1) (2009) 99–104.
- [16] K. Gu, B. Chen, Y.J. Pan, Utilization of untreated-phosphogypsum as filling and binding material in preparing grouting materials, *Constr. Build. Mater.* 265 (2020), 120749.
- [17] A.M. Rashad, Potential use of phosphogypsum in alkali-activated fly ash under the effects of elevated temperatures and thermal shock cycles, *J. Clean. Prod.* 87 (2015) 717–725.
- [18] A.P. Codinho-Castro, R.C. Testolin, L. Janke, A.X.R. Corrêa, C.M. Radetski, Incorporation of gypsum waste in ceramic block production: proposal for a minimal battery of tests to evaluate technical and environmental viability of this recycling process, *Waste Manag.* 32 (1) (2012) 153–157.
- [19] N. Deirmenci, A. Okucu, Usability of fly ash and phosphogypsum in manufacturing of building products, *J. Eng. Sci.* 2 (13) (2006) 273–278.
- [20] S. Türkel, E. Aksin, A comparative study on the use of fly ash and phosphogypsum in the brick production, *Sadhana Acad. Proc. Eng. Sci.* 37 (5) (2012) 595–607.
- [21] L. Ajam, M. Ben Ouezdou, H.S. Felfoul, R.El Mensi, Characterization of the Tunisian phosphogypsum and its valorization in clay bricks, *Constr. Build. Mater.* 23 (10) (2009) 3240–3247.
- [22] J.K. Yang, W.C. Liu, L.L. Zhang, B. Xiao, Preparation of load-bearing building materials from autoclaved phosphogypsum, *Constr. Build. Mater.* 23 (2) (2009) 687–693.
- [23] M.S. Al-Hwaiti, Assessment of the radiological impacts of treated phosphogypsum used as the main constituent of building materials in Jordan, *Environ. Earth Sci.* 74 (4) (2015) 3159–3169.
- [24] M.P. Campos, L.J.P. Costa, M.B. Nisti, B.P. Mazzilli, Phosphogypsum recycling in the building materials industry: assessment of the radon exhalation rate, *J. Environ. Radioact.* 172 (2017) 232–236.
- [25] X.B. Li, J. Du, L. Gao, S.Y. He, L. Gan, C. Sun, Y. Shi, Immobilization of phosphogypsum for cemented paste backfill and its environmental effect, *J. Clean. Prod.* 156 (2017) 137–146.
- [26] R.X. Magallanes-Rivera, C.A. Juarez-Alvarado, P. Valdez, J.M. Mendoza-Rangel, Modified gypsum compounds: an ecological-economical choice to improve traditional plasters, *Constr. Build. Mater.* 37 (2012) 591–596.
- [27] M. Singh, M. Garg, Phosphogypsum based composite binders, *J. Sci. Ind. Res.* 60 (10) (2001) 812–817.
- [28] X. Huang, X. Zhao, S. Bie, C. Yang, Hardening performance of phosphogypsum-slag-based material, *Procedia Environ. Sci.* 31 (2016) 970–976.
- [29] G. Camarini, J.A. De Milito, Gypsum hemihydrate-cement blends to improve renderings durability, *Constr. Build. Mater.* 25 (11) (2011) 4121–4125.
- [30] Y. Shen, J.S. Qian, J.Q. Chai, Y.Y. Fan, Calcium sulphoaluminate cements made with phosphogypsum: Production issues and material properties, *Cem. Concr. Compos.* 48 (2014) 67–74.
- [31] M. Singh, Treating waste phosphogypsum for cement and plaster manufacture, *Cem. Concr. Res.* 32 (7) (2002) 1033–1038.
- [32] W. Shen, G.J. Gan, R. Dong, H. Chen, Y. Tan, M.K. Zhou, Utilization of solidified phosphogypsum as Portland cement retarder, *J. Mater. Cycles Waste Manag.* 14 (3) (2012) 228–233.
- [33] M.A. Taher, Influence of thermally treated phosphogypsum on the properties of Portland slag cement, *Resour. Conserv. Recycl.* 52 (1) (2007) 28–38.
- [34] Y. Min, J.S.Qian Ying, Activation of fly ash-lime systems using calcined phosphogypsum, *Constr. Build. Mater.* 22 (5) (2008) 1004–1008.
- [35] N. Degirmenci, Utilization of phosphogypsum as raw and calcined material in manufacturing of building products, *Constr. Build. Mater.* 22 (8) (2008) 1857–1862.
- [36] Y. Huang, Z.S. Lin, Investigation on phosphogypsum-steel slag-granulated blast-furnace slag-limestone cement, *Constr. Build. Mater.* 24 (7) (2010) 1296–1301.
- [37] V.M. Pereira, R.H. Geraldo, T.A.M. Cruz, G. Camarini, Valorization of industrial by-product: Phosphogypsum recycling as green binding material, *Clean. Eng. Technol.* 5 (2021), 100310.
- [38] L. Yang, Y.S. Zhang, Y. Yan, Utilization of original phosphogypsum as raw material for the preparation of self-leveling mortar, *J. Clean. Prod.* 127 (2016) 204–213.
- [39] S. Türkel, E. Aksin, A comparative study on the use of fly ash and phosphogypsum in the brick production, *Sadhana Acad. Proc. Eng. Sci.* 37 (5) (2012) 595–607.
- [40] S.R. Saikhede, S.R. Satone, An experimental investigation of partial replacement of cement by various percentage of phosphogypsum in cement concrete, *Int. J. Eng. Sci.* 2 (4) (2012) 785–787.
- [41] M.M. Smadi, R.H. Haddad, A.M. Akour, Potential use of phosphogypsum in concrete, *Cem. Concr. Res.* 29 (9) (1999) 1419–1425.
- [42] M. Singh, M. Garg, Activation of gypsum anhydrite-slag mixtures, *Cem. Concr. Res.* 25 (2) (1995) 332–338.
- [43] Kavitha Umadevi, Studies on elevated temperature of fiber reinforced phosphogypsum concrete, *Int. J. Civ. Eng. Technol.* 7 (2) (2016) 234–246.
- [44] K. Mun, S. So, Properties of cement mortar with phosphogypsum under steam curing condition, *J. Adv. Mater. Sci. Eng.* 2008 (2016).
- [45] S. Kumar, A perspective study on fly ash-lime-gypsum bricks and hollow blocks for low cost housing development, *Constr. Build. Mater.* 16 (8) (2002) 519–525.
- [46] J.Q. Li, G.Z. Li, Y.Z. Yu, The influences of gypsum water-proofing additive on gypsum crystal growth, *Mater. Lett.* 61 (3) (2007) 872–876.
- [47] M. Singh, M. Garg, Study on anhydrite plaster from waste phosphogypsum for use in polymerised flooring composition, *Constr. Build. Mater.* 19 (1) (2005) 25–29.
- [48] W.K. Dong, W.G. Li, X.Q. Zhu, D.C. Sheng, S.P. Shah, Multifunctional cementitious composites with integrated self-sensing and hydrophobic capacities toward smart structural health monitoring, *Cem. Concr. Compos.* 118 (2021) 14.
- [49] M. Garg, M. Singh, R. Kumar, Some aspects of the durability of a phosphogypsum-lime-fly ash binder, *Constr. Build. Mater.* 10 (4) (1996) 273–279.
- [50] S. Meskini, A. Samdi, H. Ejjaouani, T. Remmal, Valorization of phosphogypsum as a road material: Stabilizing effect of fly ash and lime additives on strength and durability, *J. Clean. Prod.* 323 (2021), 129161.
- [51] M. Pang, Z.P. Sun, H.H. Huang, Compressive strength and durability of fgd gypsum-based mortars blended with ground granulated blast furnace slag, *Materials* 13 (15) (2020) 3383.
- [52] L. Xie, Y.S. Zhou, S.H. Xiao, X. Miao, A. Murzataev, D.W. Kong, L.L. Wang, Research on basalt fiber reinforced phosphogypsum-based composites based on single factor test and RSM test, *Constr. Build. Mater.* 316 (2022), 126084.
- [53] S.D. Hua, K.J. Wang, X. Yao, W. Xu, Y.X. He, Effects of fibers on mechanical properties and freeze-thaw resistance of phosphogypsum-slag based cementitious materials, *Constr. Build. Mater.* 121 (2016) 290–299.
- [54] R.S. Fu, Y.X. Lu, H.F. An, D.W. Kong, R.B. Fu, Study on preparation of cementitious materials from raw phosphogypsum cured by hemihydrate phosphogypsum and their properties, *J. Inorg. Chem. Indus* 54 (6) (2022) 109–114.
- [55] Y.S. Zhou, L. Xie, D.W. Kong, D.D. Peng, T. Zheng, Research on optimizing performance of desulfurization-gypsum-based composite cementitious materials based on response surface method, *Constr. Build. Mater.* 341 (2022), 127874.
- [56] G.Z. Jiang, A.X. Wu, Y.M. Wang, J.Q. Li, Effect of lime on properties of filling cementitious material prepared by hemihydrate, *J. Chin. Ceram. Soc.* 48 (2020) 86–93.